

ORIGINAL ARTICLE

Open Access



Size and composition of colloidal phosphorus across agricultural soils amended with biochar, manure and biogas slurry

Kamel Mohamed Eltohamy^{1,2}, Paul J. Milham³, Mostafa Gouda⁴, Daniel Menezes-Blackburn⁵, Sangar Khan¹, Boyi Liu¹, Junwei Jin¹, Ye Ye^{6*} and Xinqiang Liang^{1*}

Abstract

The long-term application of organic amendments like manure, biochar and biogas slurry can increase phosphorus (P) levels in agricultural soils; however, at present, it's not clear how this affects the P association with different mobile water-dispersible colloidal particles (P_{coll}). Thus, this study aimed to assess the effects of the long-term application of different organic amendments on the abundance, size and compositional characteristics of P_{coll} . For this purpose, a total of 12 soils amended with the above three organic amendments were sampled from the Zhejiang Province, China, and P_{coll} were fractionated into nano-sized (NC; 1–20 nm), fine-sized (FC; 20–220 nm), and medium-sized (MC; 220–450 nm) by a combination of differential centrifugation and ultrafiltration steps. These three P_{coll} forms together accounted for $74 \pm 14\%$ of the total soil solution dissolved P content, indicating that P_{coll} release was a key process in the overland P transport from these soils. Soils treated with biochar showed lower P_{coll} contents than those treated with manure or slurry alone; this effect should be further explored in a controlled inductive research approach. Compositional analysis showed that inorganic P was the predominant P_{coll} form in the NC ($54 \pm 20\%$) and FC ($63 \pm 28\%$) fractions, but not in the MC ($42 \pm 26\%$) fraction. Among the three fractions, the organic carbon (OC)–calcium (Ca) complex was the major carrier of NC-bound P_{coll} , MC-bound P_{coll} was better correlated with OC–manganese/iron/aluminium colloids than with OC–Ca colloids, and both of these phenomena co-occurred in the FC fraction. The current study provides novel insights into the impact of various carbon amendments on the propensity for P loss associated with different soil mobile colloidal fractions, and will therefore, inform future agronomic and environmental-related policies and studies.

Highlights

- Colloidal P release is a key process in the overland P transport from organic fertilised soils.
- Biochar remediates soil colloidal P content by absorbing it and improving soil aggregation.
- The composition of colloidal P in different size fractions in these soils is remarkably different.
- Organic colloidal associations with Ca were the major driver of nano-sized colloidal P content.
- Medium-size colloidal P was associated with organic colloids containing Mn/Fe/Al rather than Ca.

Handling Editor: Fangbai Li.

*Correspondence:

Ye Ye

ye200506@163.com

Xinqiang Liang

liang410@zju.edu.cn

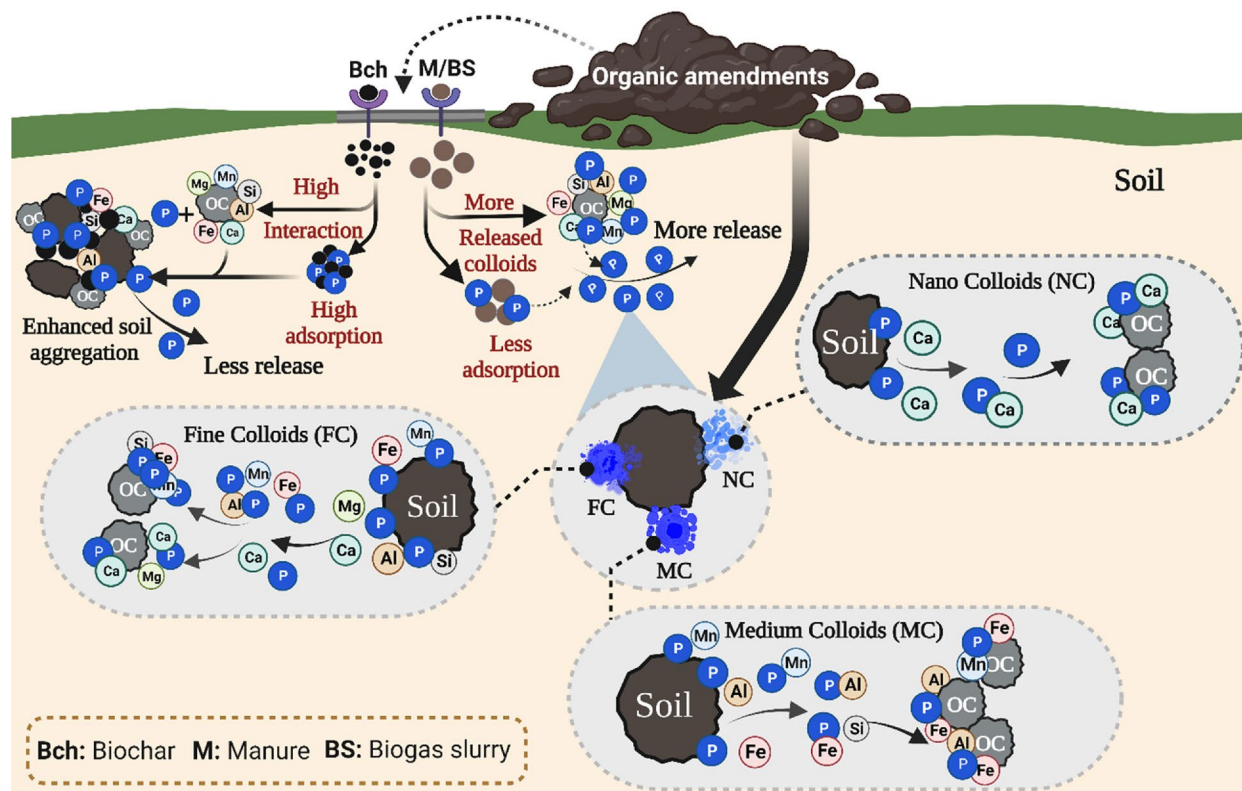
Full list of author information is available at the end of the article



© The Author(s) 2023. **Open Access** This article is licensed under a Creative Commons Attribution 4.0 International License, which permits use, sharing, adaptation, distribution and reproduction in any medium or format, as long as you give appropriate credit to the original author(s) and the source, provide a link to the Creative Commons licence, and indicate if changes were made. The images or other third party material in this article are included in the article's Creative Commons licence, unless indicated otherwise in a credit line to the material. If material is not included in the article's Creative Commons licence and your intended use is not permitted by statutory regulation or exceeds the permitted use, you will need to obtain permission directly from the copyright holder. To view a copy of this licence, visit <http://creativecommons.org/licenses/by/4.0/>.

Keywords Agricultural soils, Nano- and colloidal P, Organic carbon, Organic amendments, Biochar

Graphical Abstract



1 Introduction

Soil phosphorus (P) is a curbing nutrient in agricultural ecosystems and a major cause of surface water eutrophication (Li et al. 2021b; Jin et al. 2023). Lower P-bioavailability in agricultural soils is generally a result of its strong adsorption to soil particles or natural colloids (Menezes-Blackburn et al. 2021; Eltohamy et al. 2023b). To maintain plant growth, organic P-fertilisers have continuously been added to soils both as a source of essential nutrients and as a soil conditioner to improve overall soil fertility and health (Wang et al. 2021; Khan et al. 2022a; Zhao et al. 2022). The overuse of P-fertiliser has caused a large pool of "legacy" soil-P (Hosseini et al. 2019; Menezes-Blackburn et al. 2021). When P sufficiency is achieved, organic fertilisers are still used to address nitrogen deficiency and may correspond to continuous legacy P build-up, especially in organic fractions (Menezes-Blackburn et al. 2016b; Li et al. 2021a). This legacy-P poses a significant risk of nutrient pollution of water bodies via leaching- and runoff-related losses that are directly related

to the eutrophication of surrounding waters (Yan et al. 2016; Chen and Arai 2020; Eltohamy et al. 2021).

Natural colloids are considered important P carriers in agricultural ecosystems (Wang et al. 2020; Li et al. 2021b) and are thought to be a major cause of lower P-bioavailability to terrestrial plants (Montalvo et al. 2015). Owing to their higher surface charge and larger surface area, they remain in the soil solution for prolonged periods (Baalousha et al. 2005) and carry P to adjacent waterbodies upon irrigation or rainfall events via leaching or runoff (Jiang et al. 2015; Missong et al. 2016). These colloids contain the weathering products of minerals and the breakdown of organic matter (Missong et al. 2018; Wang et al. 2020; Eltohamy et al. 2023b). In soils amended with organic fertilisers, further colloids may originate from manure, slurry, or biochar applications (Chen and Arai 2020; Meng et al. 2021). Total colloidal P is outlined as P-containing soil particles within a size range of 1–1000 nm (Wang et al. 2020; Eltohamy et al. 2021; Khan et al. 2022b). Nonetheless,

the soil particles that have better potential to bind P are < 450 nm in size (Henderson et al. 2012; Baken et al. 2016a; Eltohamy et al. 2023b). Water-dispersible colloid-bound P (P_{coll} ; in the size range of 1–450 nm) is characterised by properties such as small size, large specific surface area, increased reactivity, and high mobility that enable its movement in a soil solution (Konrad et al. 2021; Yang et al. 2021a; Eltohamy et al. 2023b). The P_{coll} and the truly soluble P (TSP) in soil solution together represent the mobile P phase (i.e., total dissolved P; TDP) (Henderson et al. 2012; Li et al. 2021b). Nonetheless, P_{coll} has distinct colloid-chemical properties that differ from those of TSP (Henderson et al. 2012). For instance, P_{coll} may migrate more rapidly than TSP owing to the electrostatic repulsion and spatial exclusion of the soil matrix (Henderson et al. 2012; Li et al. 2021b). Several studies have documented considerably high TDP levels in soil solution and streams linked to nano (< 100 nm) and colloidal particles (< 450 nm) (Gottselig et al. 2017, 2020; Adediran et al. 2021; Li et al. 2021b). It has been reported that P_{coll} can be divided into three distinct size fractions: nano-sized colloids (NC; 1–20 nm), which are rich in organic carbon (OC), fine-sized colloids (FC; 20–220 nm), which are mainly composed of OC, iron (Fe) and aluminium (Al), and medium-sized colloids (MC; 220–450 nm), which contain a substantial quantity of phyllosilicates (Missong et al. 2018; Eltohamy et al. 2023b). Therefore, it is essential to understand how organic amendments affect the size distribution of these different P_{coll} fractions (i.e., NC, FC, and MC) and their composition. This could help us figure out the role and relative contribution of these different-sized P_{coll} fractions to P-bioavailability in these soils and their impact on soil P-cycling in terrestrial ecosystems.

To date, there are conflicting statements in the literature on the effects of long-term organic amendments on the content of soil OC and mineral elements and their relationship with the release and loss of P_{coll} from agricultural soils. Yu et al. (2017) found that organic amendments significantly increase the availability of Fe and Al minerals but decrease OC mineralisation. In contrast, Li et al. (2021b) reported a high concentration of OC in soil colloids, but a decrease in the concentrations of Fe and Al in soils amended with organic fertilisers. A study of a long-term application of manure to loam soil showed that P was associated with Ca rather than Fe or Al, leading to a transformation of relatively soluble calcium (Ca)–P into more colloidal crystal phases (Sato et al. 2005). Other studies have attributed the greater P_{coll} release in soils amended with manure to the high co-occurrence of OC_{coll} and colloidal mineral elements (i.e., Fe_{coll} , Al_{coll} , and Ca_{coll}) in these soils (Liang et al. 2016; Khan et al. 2021). It has been suggested that the

application of biochar to soils in appropriate quantities may be beneficial to avoid the risk of P_{coll} losses to adjacent waterbodies (Hosseini et al. 2019; Li et al. 2021b). For instance, straw- and manure-derived biochar effectively reduced soil P_{coll} loss by 55.2%–56.7% (Wang et al. 2023). Moreover, the addition of biochar can enhance soil phosphatase activity and promote the transformation of organic phosphate (Yang et al. 2021b; Wang et al. 2023). On the other hand, biochar contains a high content of dissolved P, a form of P that is easily lost from the soil, which can accelerate soil P loss when applied to the soil (Li et al. 2019; Eltohamy et al. 2021). Therefore, more systematic experiments on a broader scale are warranted to better investigate the associations of OC and mineral elements with P_{coll} in different colloidal size fractions in organic fertiliser-amended soils.

Therefore, we collected soil samples from 12 field sites with different organic P fertiliser application practices (i.e., manure, biochar, and biogas slurry) throughout Zhejiang Province, China, to assess the effects of long-term application of organic fertilisers on the size and compositional characteristics of P_{coll} . Our specific objectives were (a) to explore and understand the distribution of P_{coll} concentration and its contribution to TDP content in the soil solution for soils amended with organic fertilisers; (b) to probe the relative importance of P-bearing colloids of different sizes (i.e., NC, FC, and MC) and compositions on the P mobilisation and transport from these soils; and (c) to identify potential linkages between P_{coll} of different size fractions and other colloidal components at a regional-scale (Zhejiang Province, China). This study broadens our understanding of the loss behaviour of P_{coll} of different size fractions in soils amended with organic fertilisers and will help us formulate appropriate fertilisation strategies in order to reduce potential P_{coll} losses and improve its bioavailability.

2 Materials and methods

2.1 Study region and soil sampling

The soil samples used in this study were obtained from Zhejiang province in east-south China (Figure S1). This region experiences heavy rainfall (Table S1), causing soils to lose P_{coll} via runoff (Li et al. 2021b). Bulk soils (0–20 cm) were assembled from 12 field sites with organic P fertiliser application practices between October 6 and 26, 2020 (Tables S2 and S3). Sites also represented different agricultural management systems (Table S1). Each site was assigned three typical fields (three replicates). Using the S-shaped sampling technique (Wang et al. 2017), a 10 kg topsoil composite sample (10–15 subsamples) was assembled from each field and carefully mixed to generate a representative sample. The sampled

soils were then air-dried (25 ± 1 °C), coarsely crushed, and the roots and stones were eliminated. The fraction that passed through a 2-mm sieve was stored until use.

The soil samples' general properties were characterised in order to control and understand other general drivers of soil solution P_{coll} behaviour. Namely, the soil particle size distribution was determined using the hydrometric method (García-Gaines and Frankenstein 2015). The cation exchange capacity (CEC) was measured with 1 M ammonium acetate at pH 7 (Sumner and Miller 1996). Soil pH was measured at a soil-to-water ratio of 1:5 (w/v) after 30 min of shaking. The soil was digested with a nitric acid (HNO_3)–perchloric acid (HClO_4) solution plasma atomic emission and the contents of total P, Fe, Al, Ca, magnesium (Mg), and manganese (Mn) were detected using inductively coupled spectroscopy (Fresne et al. 2021). Soil total carbon was analysed by an elemental analyser (Vario MAX CNX, Elementar, Germany).

2.2 Sample processing and soil solution extraction

Figure S2 shows the analytical workflow of the study. Soils were incubated at a field-like moisture content using the method outlined earlier (Menezes-Blackburn et al. 2016b; Eltohamy et al. 2023b). First, the soils were tested to establish their maximum water-holding capacity (MWHC) by adding Milli-Q water (18.2 M Ω cm, Millipore), followed by continuous mixing until the MWHC was attained. A visual appraisal of soil plasticity and the glistening of water on the soil surface was used to figure out MWHC (Menezes-Blackburn et al. 2016a). Soil samples (150 g) were wetted with Milli-Q water to reach 50% of their MWHC. Samples were incubated at 25 ± 1 °C for 48 h and then at 100% MWHC for an additional 24 h. After incubation of the soils, the soil solutions were extracted by centrifugation at $1957 \times g$ for 15 min (Wu et al. 2018).

2.3 Colloidal size-fractionation

Differential centrifugation and ultrafiltration were used to separate colloids into three different size fractions: (1) NC (~1–20 nm, distinguishes between 300 and 3 kDa filtrates), (2) FC (~20–220 nm, distinguishes between 0.22 μm and 300 kDa filtrates), and (3) MC (220–450 nm, distinguishes between 0.45 μm and 0.22 μm filtrates), as previously described (Xia et al. 2018; Eltohamy et al. 2023b). Nitrocellulose membranes (Millipore, Billerica, Massachusetts, United States) with a pore size of 0.45 μm or 0.22 μm were used to filter out the <450 nm or <220 nm portions of the extracted soil solution. Filtration through 300- or 3-kDa ultrafiltration membranes (Millipore Amicon Ultra, United States) was used to separate the particle fraction <20 nm at $3500 \times g$ for 20 min (Xia et al. 2018) or <1 nm at $4000 \times g$ for

45 min (Li et al. 2021b). To eliminate the possibility of artifacts, ultrafiltration membranes were prewashed with 5% HNO_3 (v/v) and then rinsed three times with Milli-Q water (Saeed et al. 2018). The association between the used molecular weight cut-offs and membrane particle size cut-offs has been previously validated (Henderson et al. 2012; Xia et al. 2018; Li et al. 2021b). The estimation was done based on the relationship between Stokes diameter and both molecular weight and molecular shape of organic test macromolecules (Xia et al. 2018).

Total P, Al, Fe, Ca, Mg, silicon (Si), and Mn concentrations were determined with an inductively coupled plasma-mass spectrometer (ICP-MS, Agilent 7800, Agilent Technologies, Santa Clara, CA, United States) in a subset of the filtrates (i.e., 0.45 μm , 0.22 μm , 300 kDa, and 3 kDa) acidified to pH 2 with 1 M HNO_3 . The internal standard was a Rhodium (^{103}Rh) solution (GSS2; National Sharing Platform for Reference Material, China). After acidification (pH < 2) with 0.5 M hydrochloric acid (HCl), the total OC concentrations of the filtrates were measured using a total OC analyser (multi N/C2100, Analytik Jena, Germany). The quality control of these analytical analyses was validated in our prior study (Eltohamy et al. 2023b). To verify the effective size fractionation of the mobile colloids in the extracted soil solution (Figure S2), dynamic light scattering (DLS) measurements were performed on the non-acidified <450 nm portions using the Zetasizer (Nano-ZS, Malvern Panalytical, Worcestershire, United Kingdom).

2.4 Determination of inorganic and organic phosphorus forms in dissolved and colloidal phases

The P concentrations in the 0.45 μm and 3 kDa filtrates measured by ICP-MS indicate TDP and TSP, respectively. The concentration of dissolved molybdate-reactive P (i.e., dissolved inorganic P; DPI) was measured colorimetrically (Murphy and Riley 1962) using part of the unacidified 0.45 μm filtrate. Dissolved molybdate-unreactive P (i.e., dissolved organic P; DPO) was estimated as the difference between TDP and DPI . Additionally, the colloidal molybdate-reactive P_{coll} (inorganic P_{coll} ; Pi_{coll}) concentration was measured on the unacidified portions of all filtrates by reaction with molybdate (Murphy and Riley 1962) and the colloidal molybdate-unreactive P (organic P_{coll} ; Po_{coll}) was calculated by subtracting Pi_{coll} from P_{coll} .

2.5 Statistical analysis

Significant differences in the independent variables between soils were assessed using a one-way analysis of variance, and the means were compared using Tukey's multiple comparison test ($p < 0.05$). Pearson correlation coefficients were computed between the independent variables, and the significance of correlations was

determined using Student's *t*-test (significant at $p \leq 0.05$ and highly significant at $p \leq 0.01$). The correlation coefficients were calculated with log-transformed data to minimise heteroskedasticity. Principal component analysis (PCA) scores and model cross-validation (Q^2) were calculated using partial least squares-discriminant multivariate analysis (PLS-DA). Data processing and analysis were performed with Microsoft Excel and SPSS statistical software package ver. 22 (SPSS Inc., Chicago, IL). Visualisation was conducted using OriginPro 2021 (OriginLab Corp., United States).

3 Results and discussion

3.1 General characteristics of the tested soils

Table 1 shows the general characteristics of the tested soils. The soil pH varied between acidic (4.58; S12) and alkaline (7.96; S9). Soil content of total carbon ranged from 5.62 g kg⁻¹ in S3 soil to 27.27 g kg⁻¹ in S11 soil. Soil total P content was the highest in the S2 soil (4.94 g kg⁻¹) and the lowest in the S10 soil (0.38 g kg⁻¹). The highest total Fe (32.14 g kg⁻¹), total Al (41.08 g kg⁻¹), and total Mg (9.92 g kg⁻¹) contents were also found in S2 soil, whereas the lowest contents were 7.49 g kg⁻¹ for total Fe in S12 and 9.61 g kg⁻¹ for total Al and 0.94 g kg⁻¹ for total Mg in S11 soil. The soils had much lower contents of total Mn (0.12 (S12)–0.97 (S7) g kg⁻¹). The highest soil total Ca content occurred in S9 (8.22 g kg⁻¹) and the lowest was in S12 (0.93 g kg⁻¹). The CEC varied greatly among the soils, ranging from 11.22 cmol kg⁻¹ (S3) to 166.71 cmol kg⁻¹ (S10). The results showed a strong variation in the spatial distribution of the general characteristics of the studied soils (Table 1), indicating that the soils in central and southern Zhejiang are rich in Fe and Al and contain less carbon (Table 1 and Figure S1). The soils in the northern plain showed lower Al, distinct

accumulation layers, as well as greater carbon storage and clay content (Table 1). Similar results were found by previous work from our group, (Li et al. 2021b; Eltohamy et al. 2023b), using the same study areas. These observed patterns, and heterogeneity of regional differences in the observed background properties of the soils, allow for contrasting different response parameters with the colloidal sizes and their compositional distribution patterns of these soils.

3.2 Partitioning of soil solution P between colloidal and dissolved phases of the studied soils

The total dissolved P in soil solution (i.e., TDP) consists of P_{coll} (<450 nm) and TSP (Henderson et al. 2012; Li et al. 2021b). The studied soils had a wide range of TDP contents (123.5 (S12)–2826.3 (S2) mg L⁻¹; Table S4) and were dominated by DPi (mean \pm SD = 68 \pm 13% of TDP; Fig. 1A). Such a high presence of DPi in the soil solution on account of DPo implied a high P-bioavailability in the studied soils. This is because the DPi represents the soil solution labile P pool that compensates for the P depleted by plant uptake from the root zone (Eltohamy et al. 2023b). DPo, on the other hand, is not readily available for plant uptake as it has a high molecular weight and needs to be digested and made available in the form of orthophosphate, a soluble inorganic P form (Das et al. 2022).

P_{coll} represented a higher average proportion of TDP than TSP (P_{coll} = 73 \pm 14% vs. TSP = 27 \pm 14%; Fig. 1B and Tables 2 and S5), indicating that the potential risk of TDP transport from organic fertiliser-amended soils to adjacent waters often takes place in the colloidal phase. The higher proportion of P_{coll} relative to TSP also suggests that P-containing colloids may be resedimented during transport through soil macropores, which act as

Table 1 Summary of the tested soil characteristics

Site	pH	TC g kg ⁻¹	TP g kg ⁻¹	TFe g kg ⁻¹	TAI g kg ⁻¹	TMg g kg ⁻¹	TCa g kg ⁻¹	TMn g kg ⁻¹	CEC cmol kg ⁻¹	Sand %	Silt %	Clay %
S1	6.31	10.94	2.11	29.11	36.42	7.15	1.97	0.87	72.51	39.32	18.29	42.39
S2	5.54	7.45	4.94	32.14	41.08	9.92	4.33	0.64	13.35	33.87	41.64	24.49
S3	5.83	5.62	4.39	25.24	37.56	6.34	6.92	0.86	11.22	46.21	17.92	35.87
S4	5.20	11.26	1.35	19.72	23.79	2.15	1.44	0.22	95.80	51.76	14.69	33.55
S5	5.36	9.73	2.73	23.20	21.35	5.26	2.07	0.47	105.34	16.39	42.79	40.82
S6	4.72	12.02	1.25	24.22	20.25	1.67	1.28	0.43	129.40	57.23	29.41	13.36
S7	7.54	14.67	2.31	28.15	32.52	5.89	4.13	0.97	32.53	15.65	43.72	40.63
S8	6.75	6.25	1.52	16.62	21.16	5.62	3.16	0.42	18.72	41.26	23.57	35.17
S9	7.96	11.24	1.88	19.04	23.16	6.27	8.22	0.60	27.45	17.95	67.12	14.93
S10	7.23	22.78	0.38	14.49	12.53	3.53	1.74	0.51	166.71	41.48	45.25	13.27
S11	7.33	27.27	1.85	13.12	9.61	0.94	3.82	0.13	25.83	43.74	40.33	15.93
S12	4.58	25.93	0.87	7.49	10.72	1.87	0.93	0.12	124.11	16.75	72.38	10.87

TC total carbon, TP total phosphorus, TFe total iron, TAI total aluminium, TMg total magnesium, TCa total calcium, TMn total manganese, CEC cation exchange capacity

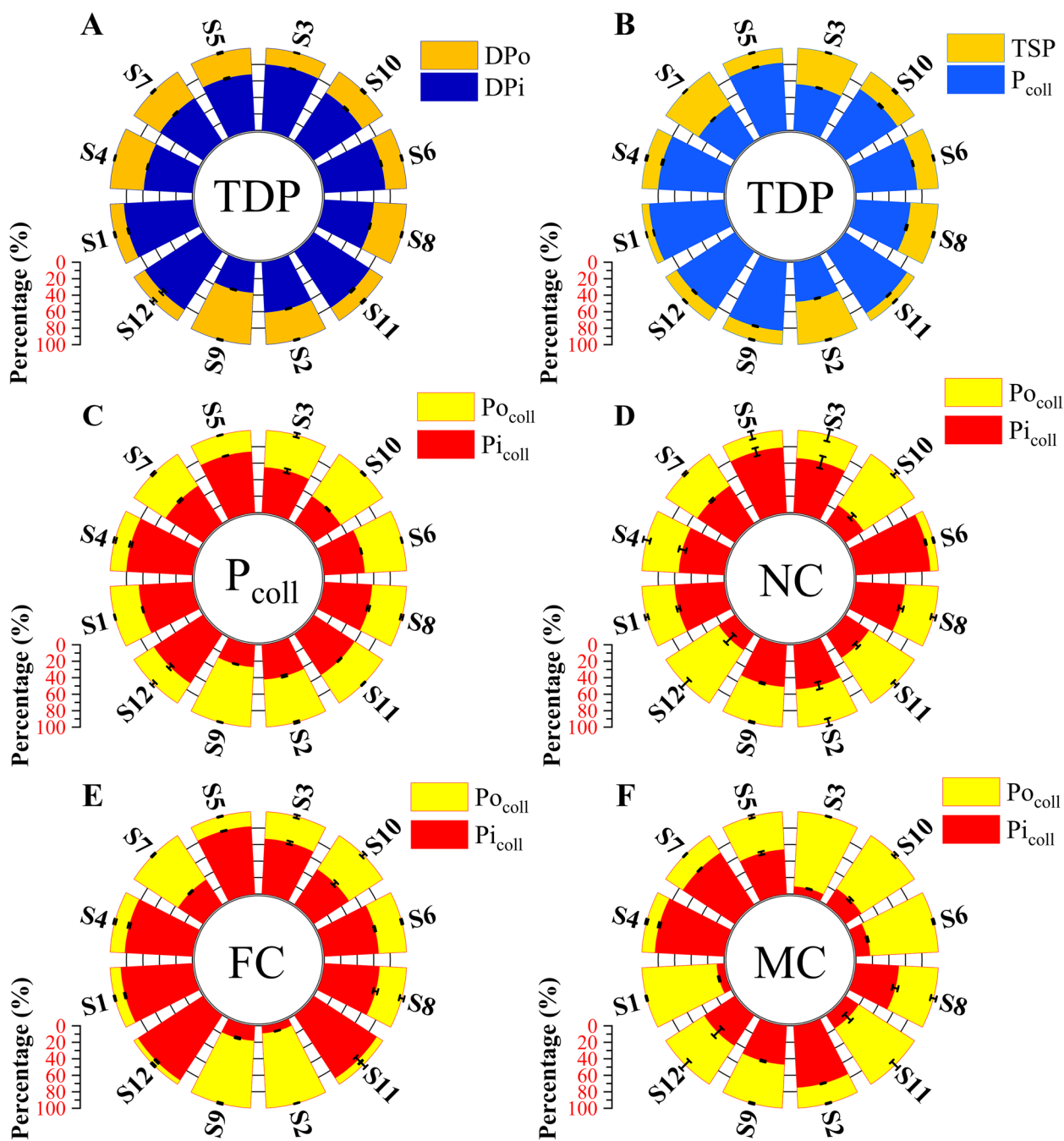


Fig. 1 Partitioning of total dissolved P (TDP) in soil solution between (A) dissolved inorganic P (DPI; in % of TDP) and dissolved organic P (DPO; in % of TDP) and between (B) colloidal P (P_{coll} ; in % of TDP) and truly soluble P (TSP; in % of TDP) and the distribution of P_{coll} between inorganic P_{coll} (Pi_{coll} ; in % of P_{coll}) and organic P_{coll} (Po_{coll} ; in % of P_{coll}) in the size ranges (C) total (1 – 450 nm), (D) nano (NC; 1 – 20 nm), (E) fine (FC; 20 – 220 nm), and (F) medium colloids (MC; 220 – 450 nm)

preferential flow pathways for TDP (Julich et al. 2017; Gu et al. 2020). This is consistent with previous studies which concluded that 40–58% of TDP transport from the topsoil profile is in the form of P_{coll} (Hens and Merckx 2002; Wang et al. 2021).

The results also showed that spatial distribution characteristics of the tested soils (Tables 1 and S1) probably influenced the P_{coll} content in the soil solution (Table 2). The P_{coll} in the soil solution can be categorised into the concentration ranges, low (103.6 (S12) to

Table 2 Mean concentrations of colloidal P (P_{coll} ; $\mu\text{g L}^{-1}$), inorganic P ($P_{\text{i coll}}$; $\mu\text{g L}^{-1}$), and organic P ($P_{\text{o coll}}$; $\mu\text{g L}^{-1}$) in the nano-sized (1–20 nm), fine-sized (20–220 nm), and medium-sized (220–450 nm) fractions in the soil solution of tested soils ($n = 3$)

Sites	1–20 nm			20–220 nm			220–450 nm			Sum of fractions		
	P_{coll}	$P_{\text{i coll}}$	$P_{\text{o coll}}$	P_{coll}	$P_{\text{i coll}}$	$P_{\text{o coll}}$	P_{coll}	$P_{\text{i coll}}$	$P_{\text{o coll}}$	P_{coll}	$P_{\text{i coll}}$	$P_{\text{o coll}}$
S1	113.4 ^b	67.7 ^b	45.7 ^b	1391.4 ^a	1216.1 ^a	175.3 ^c	536.6 ^a	48.9 ^{cd}	487.7 ^a	2041.4 ^a	1332.7 ^a	708.7 ^b
S2	154.9 ^a	82.9 ^b	72.0 ^a	633.4 ^b	59.1 ^d	574.3 ^a	570.6 ^a	428.4 ^a	142.2 ^c	1358.9 ^b	570.4 ^b	788.5 ^a
S3	167.9 ^a	110.8 ^a	57.1 ^{ab}	673.7 ^b	454.4 ^b	219.3 ^b	212.0 ^b	18.6 ^{de}	193.4 ^b	1053.6 ^c	583.8 ^b	469.8 ^c
S4	36.7 ^{cd}	20.3 ^{cd}	16.4 ^{cd}	278.8 ^c	228.4 ^c	50.4 ^e	162.5 ^{bc}	135.7 ^b	26.8 ^f	478.0 ^d	384.4 ^c	93.6 ^{defg}
S5	26.3 ^{cd}	20.8 ^{cd}	5.5 ^d	214.2 ^{cd}	175.7 ^c	38.5 ^{ef}	88.3 ^{de}	47.9 ^{cd}	40.4 ^{ef}	328.8 ^{de}	244.4 ^d	84.4 ^{fg}
S6	40.3 ^{cd}	36.4 ^c	3.9 ^d	146.8 ^{de}	97.1 ^d	49.7 ^e	128.4 ^{cd}	21.6 ^{de}	106.8 ^d	315.5 ^{de}	155.1 ^{de}	160.4 ^{de}
S7	48.2 ^c	25.8 ^{cd}	22.4 ^c	105.3 ^e	38.3 ^d	67.0 ^e	86.6 ^{de}	65.0 ^c	21.6 ^f	240.1 ^e	129.1 ^e	111.0 ^{def}
S8	28.9 ^{cd}	17.1 ^{cd}	11.8 ^{cd}	76.6 ^e	51.2 ^d	25.4 ^{ef}	127.7 ^{cd}	66.0 ^c	61.7 ^e	233.2 ^e	134.3 ^e	98.9 ^{defg}
S9	37.4 ^{cd}	19.2 ^{cd}	18.2 ^{cd}	161.6 ^{de}	29.4 ^d	132.2 ^d	28.7 ^{ef}	13.5 ^{de}	15.2 ^f	227.7 ^e	62.1 ^e	165.6 ^d
S10	29.4 ^{cd}	7.6 ^d	21.8 ^c	80.2 ^e	40.6 ^d	39.6 ^{ef}	32.4 ^{ef}	7.5 ^e	24.9 ^f	142.0 ^f	55.7 ^e	86.3 ^{efg}
S11	36.5 ^{cd}	12.3 ^{cd}	24.2 ^c	63.6 ^e	57.8 ^d	5.8 ^f	26.7 ^f	5.2 ^e	21.5 ^f	126.8 ^f	75.3 ^e	51.5 ^{fg}
S12	20.2 ^d	4.7 ^d	15.5 ^{cd}	63.6 ^e	59.8 ^d	3.8 ^f	19.8 ^f	8.7 ^e	11.1 ^f	103.6 ^f	73.2 ^e	30.4 ^g

Lowercase letters indicate significant differences in the independent variables among the soils at $p < 0.05$

142.0 $\mu\text{g L}^{-1}$ (S10)), moderate (227.7 (S9) to 478.0 $\mu\text{g L}^{-1}$ (S4)), and high (1053.6 (S3) to 2041.4 $\mu\text{g L}^{-1}$ (S1)) (Table 2). Soils in central and southern Zhejiang had moderate to high P_{coll} levels (S1–S9). This could be due to the fact that the soils in the central and southern plains are highly susceptible to desilication, are rich in Fe and Al, and contain less carbon (Table 1) (Zhejiang Soil Census Office 1994), resulting in high P_{coll} release into the soil solution. While the northern plain soils have lower aluminium content, higher carbon storage and clay content (Table 1) (Zhejiang Soil Census Office 1994; Li et al. 2021b), result in low P_{coll} release (S10–S12). This pattern causes regional differences in the distribution patterns of P_{coll} as previously hypothesized (Li et al. 2021b).

3.3 Compositional characteristics of colloidal phosphorus of different size fractions

There were obvious differences in the contents of the three colloidal fractions between soils (Tables 2, 3 and S6). Note that the soils were ordered according to their soil solution P_{coll} content, with S1 soil (2041.4 $\mu\text{g L}^{-1}$) having the greatest content and S12 soil having the lowest (103.6 $\mu\text{g L}^{-1}$) (Table 2). As shown by the DLS measurement (Fig. 2), the effective particle size of the 450-nm extracted soil solution ranged from 176.6 ± 47.7 (S1) to 352.3 ± 27.1 nm (S10). This indicates that most of the mobile colloids of the studied soils were distributed among the FC and MC fractions. On average, the size distribution of P_{coll} was predominantly present as FC (322.4 $\mu\text{g L}^{-1}$), compared to MC (168.4 $\mu\text{g L}^{-1}$) and NC (61.7 $\mu\text{g L}^{-1}$) (Table 2). P_{coll} was enriched in inorganic P ($P_{\text{i coll}} = 56 \pm 15\%$ of P_{coll} ; Fig. 1C). However, the

partitioning of P_{coll} between inorganic and organic P ($P_{\text{i coll}}$ vs. $P_{\text{o coll}}$) appears to vary among the three colloidal fractions and shows different patterns in the speciation distribution of P_{coll} (Figs. 1D–F). On average, NC- and FC-bound P_{coll} made up $54 \pm 20\%$ and $63 \pm 28\%$ of $P_{\text{i coll}}$, respectively (Figs. 1D and E). In contrast, MC-bound P_{coll} was more enriched in $P_{\text{o coll}}$ ($58 \pm 26\%$; Fig. 1F). This shows that NC- and FC-bound P_{coll} fractions are more bioavailable than the MC-bound P_{coll} fraction. This result supports the hypothesis of a recent study that NC- and FC-bound P_{coll} can contribute to P uptake, whereas MC-bound P_{coll} is involved in vertical P-transport from the soil solution and leads to P enrichment in receiving waters (Eltohamy et al. 2023b).

Total OC_{coll} was the main constituent of the colloids suspended in the soil solution (Fig. 3), and its mean concentrations in FC (28.5 mg L^{-1}) or MC (14.9 mg L^{-1}) were far below those in NC (35.4 mg L^{-1}) (Table 3). This suggests that NC-bound OC_{coll} is an important source of OC transfer in soils amended with organic fertilisers (Menezes-Blackburn et al. 2021; Eltohamy et al. 2023b). Other colloidal constituents were predominantly distributed in the FC or MC (Fig. 3 and Table 3), showing that these elements are important units for the formation of larger colloids (Wang et al. 2020). The size distributions of Al_{coll} and Fe_{coll} were very similar (Fig. 3), revealing that Al_{coll} might be present as Al-oxyhydroxides associated with the Fe-oxyhydroxide colloids (Baken et al. 2016b). The OC-rich composition of the NC fraction (Fig. 3) agrees well with previous studies for P-bearing nanoparticles in an Albeluvisol and a Stagnosol (Jiang et al. 2017; Gu et al. 2020). According to Jiang

Table 3 Mean concentration of colloidal organic carbon (OC_{coll}), aluminium (Al_{coll}), iron (Fe_{coll}), magnesium (Mg_{coll}), calcium (Ca_{coll}), silicon (Si_{coll}), and manganese (Mn_{coll}) in nano-sized (1–20 nm), fine-sized (20–220 nm), and medium-sized (220–450 nm) fractions in the soil solution of tested soils (n = 3)

Sites	1–20 nm (mg L ⁻¹)							20–220 nm (mg L ⁻¹)							220–450 nm (mg L ⁻¹)						
	OC _{coll}	Al _{coll}	Fe _{coll}	Mg _{coll}	Ca _{coll}	Si _{coll}	Mn _{coll}	OC _{coll}	Al _{coll}	Fe _{coll}	Mg _{coll}	Ca _{coll}	Si _{coll}	Mn _{coll}	OC _{coll}	Al _{coll}	Fe _{coll}	Mg _{coll}	Ca _{coll}	Si _{coll}	Mn _{coll}
S1	80.5 ^a	3.5 ^a	3.9 ^a	2.6 ^a	2.6 ^b	1.9 ^a	0.7 ^a	94.7 ^a	17.6 ^a	15.7 ^a	8.0 ^{ab}	3.9 ^a	2.9 ^a	2.0 ^a	58.8 ^a	4.0 ^a	4.9 ^a	7.0 ^{bc}	1.1 ^{bc}	2.4 ^a	1.2 ^b
S2	28.4 ^{cd}	0.9 ^{bc}	0.8 ^{cd}	1.1 ^d	4.1 ^a	0.6 ^c	0.5 ^{bc}	34.0 ^c	3.4 ^c	3.8 ^c	7.1 ^b	2.7 ^{bc}	2.8 ^a	2.1 ^a	24.7 ^c	2.7 ^b	3.0 ^b	11.3 ^a	4.2 ^a	1.4 ^b	2.5 ^a
S3	67.4 ^b	0.5 ^{bc}	0.6 ^d	1.4 ^{cd}	0.5 ^d	0.6 ^c	0.4 ^{de}	20.5 ^d	1.9 ^{cd}	1.5 ^{de}	9.4 ^a	3.3 ^{ab}	1.4 ^{bc}	2.3 ^a	8.6 ^{de}	1.3 ^d	1.0 ^{de}	8.0 ^b	1.2 ^b	1.0 ^c	0.9 ^c
S4	13.9 ^{ef}	0.4 ^{bc}	0.9 ^c	1.4 ^{cd}	0.9 ^c	0.4 ^c	0.6 ^{ab}	23.0 ^d	6.4 ^b	4.7 ^{bc}	5.2 ^c	1.7 ^{de}	1.2 ^{cd}	1.0 ^b	5.7 ^e	2.7 ^b	3.1 ^b	3.3 ^{ef}	0.5 ^e	0.5 ^d	0.7 ^d
S5	34.9 ^c	0.8 ^{bc}	1.2 ^b	1.7 ^{bc}	0.5 ^d	0.3 ^c	0.4 ^{de}	72.1 ^b	5.7 ^b	5.1 ^b	2.8 ^{de}	0.9 ^g	0.8 ^{ef}	0.9 ^{bc}	16.0 ^{cd}	1.5 ^{cd}	1.4 ^{cd}	6.9 ^{bc}	0.7 ^d	0.6 ^d	0.5 ^{ef}
S6	67.3 ^b	0.3 ^c	0.3 ^e	0.4 ^e	0.5 ^d	1.0 ^b	0.4 ^{cd}	19.9 ^{de}	0.9 ^d	0.5 ^e	1.6 ^{ef}	0.4 ^g	1.5 ^b	1.0 ^b	11.0 ^{de}	0.7 ^{ef}	0.4 ^f	0.7 ^g	0.4 ^{ef}	1.4 ^b	0.6 ^{de}
S7	21.0 ^{de}	0.5 ^c	0.3 ^e	0.4 ^e	0.5 ^d	0.4 ^c	0.2 ^f	19.5 ^{de}	0.6 ^d	0.6 ^{ef}	2.4 ^{ef}	1.3 ^{ef}	0.3 ^g	0.5 ^{cd}	6.2 ^e	0.5 ^f	0.6 ^{ef}	5.7 ^{cd}	0.4 ^{ef}	0.4 ^d	0.3 ^g
S8	68.4 ^b	1.0 ^b	1.0 ^{bc}	1.8 ^b	0.6 ^d	0.6 ^{bc}	0.5 ^{bc}	24.9 ^{cd}	3.1 ^c	2.5 ^d	2.8 ^{de}	2.1 ^{cd}	1.0 ^{de}	1.1 ^b	35.0 ^b	1.8 ^c	1.6 ^c	4.8 ^{de}	1.0 ^c	0.7 ^{cd}	0.4 ^g
S9	12.3 ^{ef}	0.5 ^{bc}	0.2 ^e	1.2 ^d	1.1 ^c	0.5 ^c	0.3 ^{def}	14.8 ^e	1.1 ^d	0.3 ^f	1.6 ^{ef}	2.1 ^{cd}	0.8 ^{ef}	0.4 ^d	4.4 ^e	1.1 ^{de}	0.3 ^f	6.3 ^{bcd}	1.2 ^b	0.7 ^{cd}	0.4 ^g
S10	13.4 ^{ef}	0.4 ^c	0.3 ^e	1.2 ^d	0.6 ^d	0.7 ^{bc}	0.6 ^{ab}	15.6 ^{de}	1.1 ^d	0.6 ^{ef}	2.7 ^{de}	0.5 ^g	1.7 ^b	1.0 ^b	3.7 ^e	0.5 ^f	0.5 ^{ef}	1.6 ^g	0.5 ^e	0.9 ^c	0.8 ^{cd}
S11	6.6 ^f	0.6 ^{bc}	0.2 ^e	1.1 ^d	0.5 ^d	0.3 ^c	0.3 ^{ef}	1.0 ^f	0.9 ^d	0.3 ^f	4.3 ^{cd}	0.8 ^g	0.6 ^g	0.6 ^{cd}	2.9 ^e	0.7 ^{ef}	0.2 ^f	7.8 ^b	0.5 ^e	0.5 ^d	0.5 ^{ef}
S12	11.1 ^{ef}	0.8 ^{bc}	0.3 ^e	0.4 ^e	0.2 ^d	0.6 ^c	0.3 ^f	2.2 ^f	0.8 ^d	0.5 ^{ef}	0.8 ^f	0.3 ^g	0.8 ^{def}	0.3 ^d	2.5 ^e	0.5 ^f	0.5 ^{ef}	1.1 ^g	0.2 ^f	0.9 ^c	0.3 ^g

Lowercase letters indicate significant differences in the independent variables among the soils at $p < 0.05$

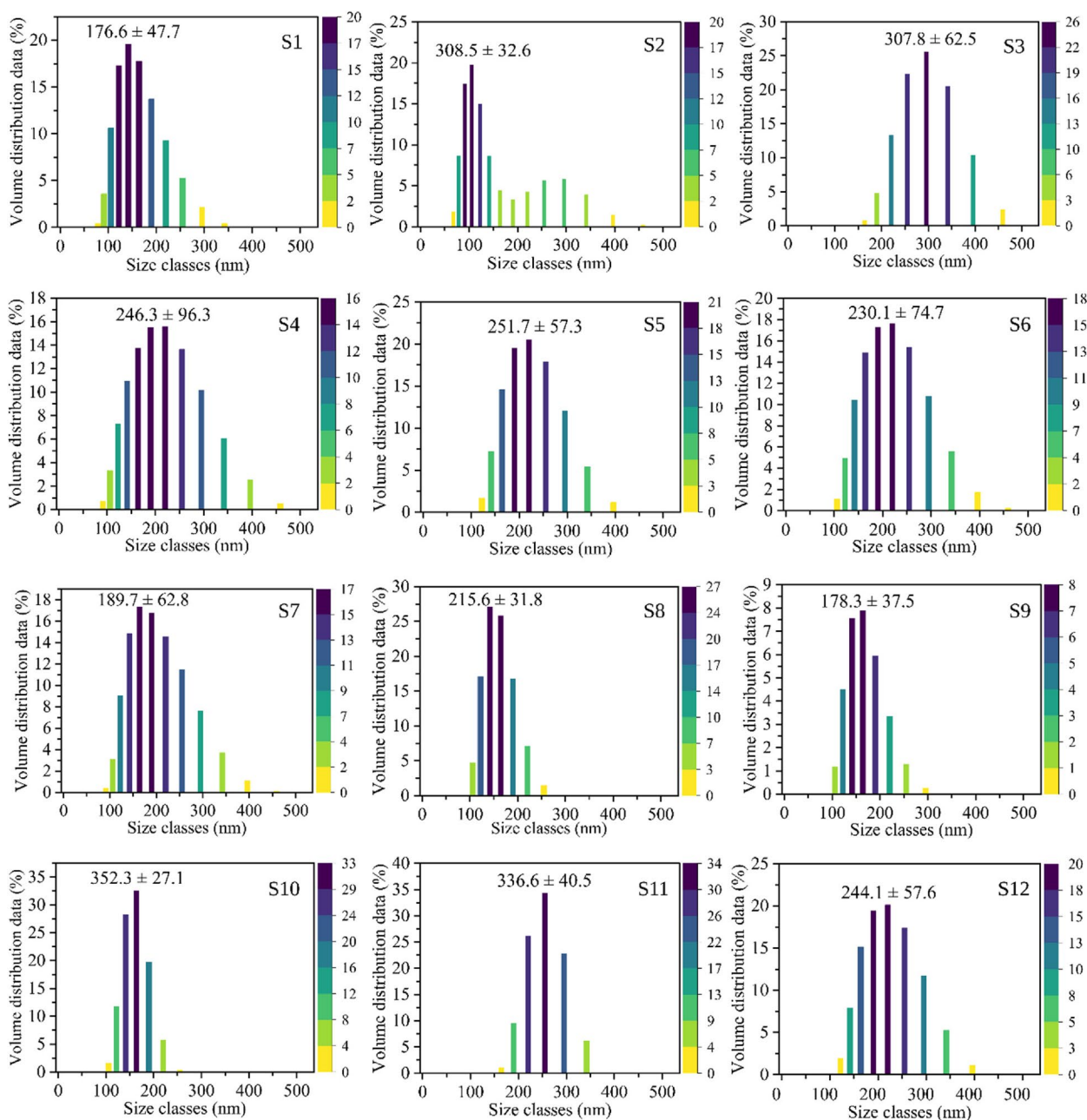


Fig. 2 Particle distribution of soil solution colloids (<450 nm) in the tested soils

et al. (2017), the reduction regime that characterises waterlogged soils (as in the present study, in which the soils were moistened to their MWHC) explains this difference in the composition of P-bearing colloids. These two factors would favor the formation of OC-dominated nanoparticles with a minor contribution of other colloidal components. The abundant presence of OC in both NC and FC relative to the MC could also be a reason for the better bioavailability

of NC- and FC-bound P_{coll} fractions than MC-bound P_{coll} . This is because organic matter attached to the particle surface facilitates the dispersibility of these colloids in the soil solution by changing their surface charges to be more negative (Missong et al. 2018; Eltohamy et al. 2023a). This, in turn, leads to the dissolution or desorption of these NC- and FC-bound P_{coll} fractions and thus causes diffusion near the plant root (Eltohamy et al. 2023b).

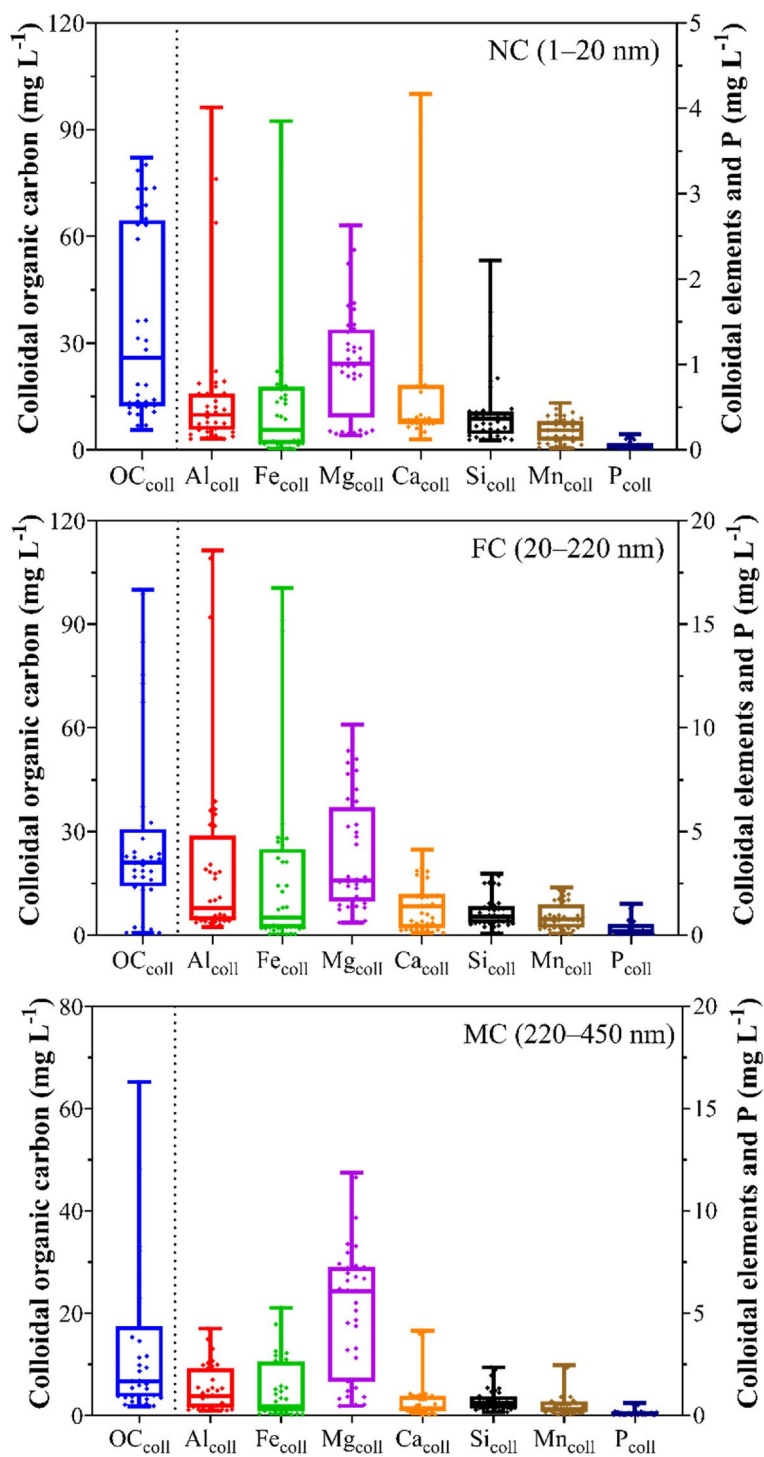


Fig. 3 Concentrations of colloidal phosphorus (P_{coll}) and other colloidal components in the nano- (NC; 1–20 nm), fine- (FC; 20–220 nm), and medium-sized (MC; 220–450 nm) fractions. Dots represent individual values ($n = 36$)

3.4 Association of colloidal phosphorus of different size fractions with other colloidal components

The relationships between P_{coll} in the three colloidal fractions, and the other colloidal components, are shown in

Fig. 4A. The variances by multivariate principal component analysis showed significant discrimination ($p < 0.05$) among the concentrations of different-size colloids in the 12 tested soils based on the first two components, which

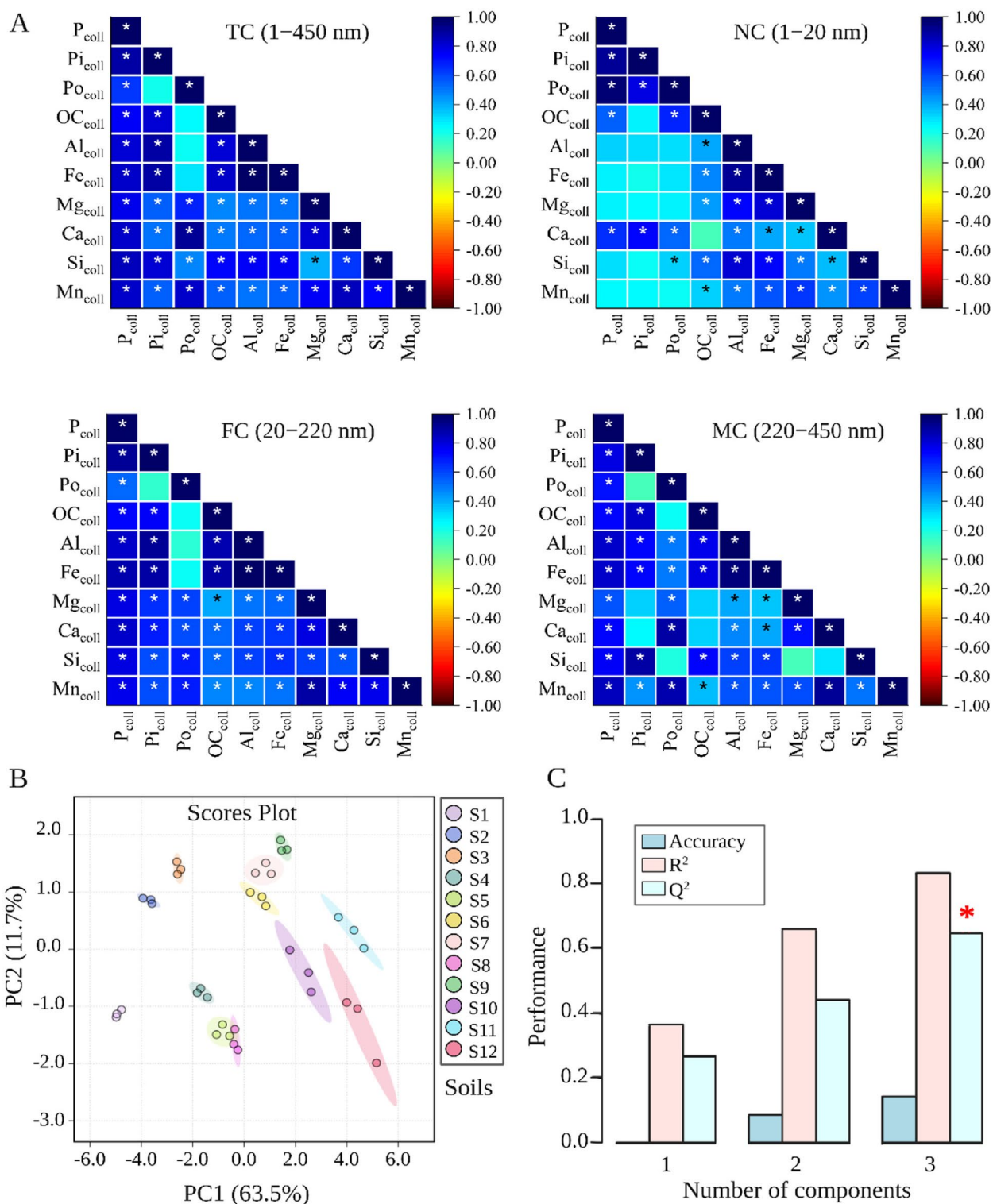


Fig. 4 Pearson correlation coefficients (A) principal component analysis (PCA) (B), and model performance (C) of colloidal P forms (P_{coll} , Pi_{coll} , Po_{coll}) with other colloids (OC_{coll} , Fe_{coll} , Al_{coll} , Mg_{coll} , Ca_{coll} , Si_{coll} , and Mn_{coll}) at nano- (NC; 1–20 nm), fine- (FC; 20–220 nm), and medium-sized (MC; 220–450 nm) fractions

accounted for 75.2% of the total variance (Fig. 4B), and the greater the range, the lower the bias in the correlation analysis. Additionally, the experimental PCA model showed high prediction based on the PLS-DA model indicators for the second PC ($Q^2 > 0.5$) (Fig. 4C). That is, the model had a strong predictive ability based on the first two principal components (Szymańska et al. 2012).

The elemental composition of these colloids showed that OC_{coll} , Al_{coll} , Fe_{coll} , Mg_{coll} , Ca_{coll} , Si_{coll} , and Mn_{coll} were strongly correlated with P_{coll} ($r \geq 0.76$; Fig. 4A and Table S7). These correlations support the previous suggestion that mobile P_{coll} tends to be associated with OC–elemental species containing Fe, Al, Ca, Mg, Mn, and Si (Konrad et al. 2021; Li et al. 2021b; Eltohamy et al. 2023b). Here, our results show that NC-bound P_{coll} was correlated only with the OC–Ca colloids ($r \geq 55$; Fig. 4A and Table S7) that presumably dominated by organic compounds stabilised by bridging Ca^{2+} ions (Fig. 5), which are stable enough to avoid hetero-aggregation with other colloidal soil particles (Li et al. 2021b; Eltohamy et al. 2023b). In contrast, MC-bound P_{coll} was better associated with Mn/

Fe/Al colloids ($r = 0.82$ to 0.86) complexed with OC_{coll} ($r = 0.74$) than OC–Ca colloids ($r = 0.59$ for Ca_{coll} ; Fig. 4A and Table S7). Previous investigations on natural and laboratory-extracted colloids in the range of 160 nm to 450 nm have also shown the importance of metal oxyhydroxides (e.g., Fe/Al-oxyhydroxides) and organic matter as effective P adsorption sinks (Jiang et al. 2015; Yan et al. 2016; Gu et al. 2020). Therefore, we can assume that the P-bearing colloidal vectors in the MC fraction are largely colloidal Fe/Al/Mn-oxyhydroxides complexed with OC_{coll} (Fig. 5). FC-bound P_{coll} was highly correlated with all other colloidal components ($r = 0.73$ to 0.86 ; Fig. 4A and Table S7) suggesting that two phenomena (OC–Ca–P and OC–Mn/Fe/Al–P) were occurring in this size range (i.e., FC; 20–220 nm) (Fig. 5). Thus, we can conclude that the OC–Ca complex was the major carrier of NC-bound P_{coll} , OC–Mn/Fe/Al colloids were the main vectors of MC-bound P_{coll} , and these two phenomena (i.e., OC–Ca–P and OC–Mn/Fe/Al–P) co-occurred in the FC fraction.

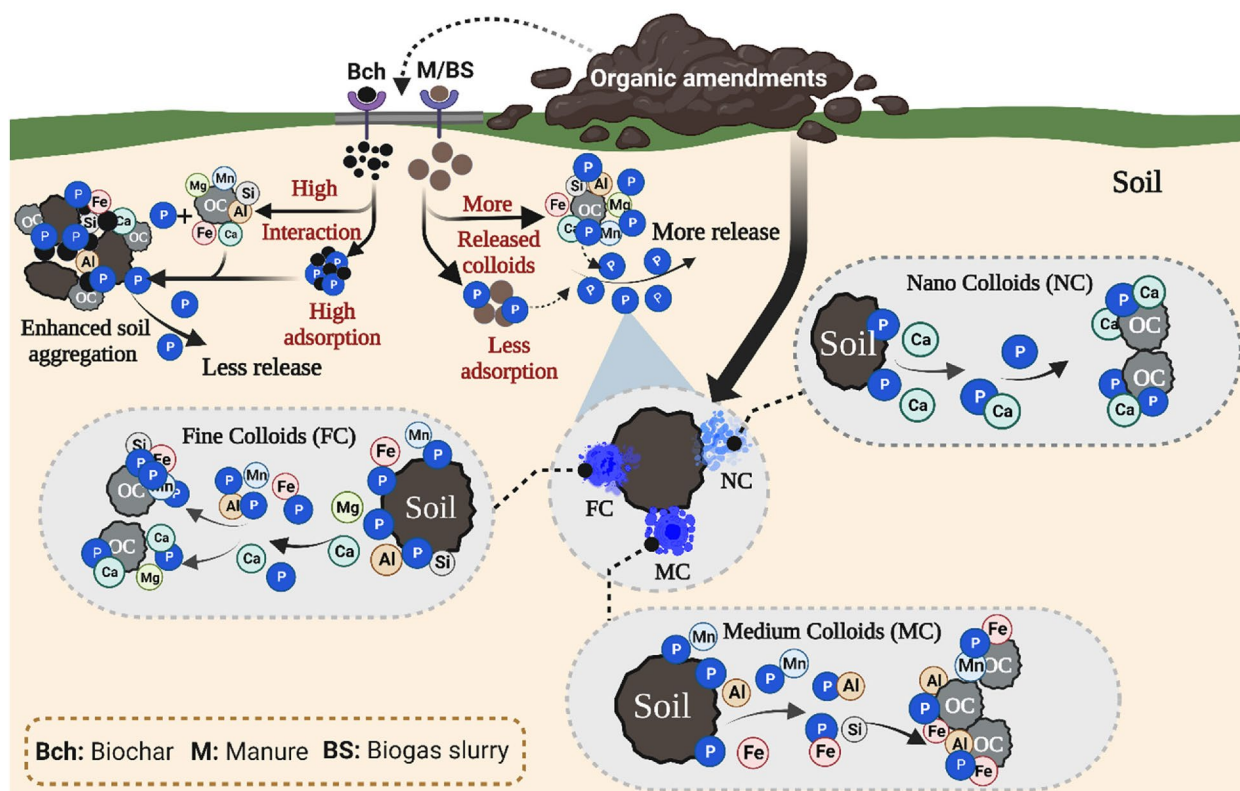


Fig. 5 Mechanisms of in-soil micro-scale release and migration of colloids at nano- (NC; 1–20 nm), fine- (FC; 20–220 nm), and medium-sized (MC; 220–450 nm) fractions in soils amended with organic fertilisers

3.5 Effect of biochar amendment on colloidal phosphorus content and size distribution versus other organic amendments

The soils to which manure or biogas slurry was added, i.e., soils S1 to S6, had higher P_{coll} concentrations (Tables 2 and S2), and this result was consistent with recent works on natural and laboratory-extracted soil colloids (Niyungeko et al. 2018; Eltohamy et al. 2021; Li et al. 2021b; Khan et al. 2022a). Li et al. (2021a, b) observed that the application of biogas slurry, instead of 30% chemical fertiliser, considerably enhanced soil P_{coll} . They attributed this to the possibility that the biogas slurry itself contained a large amount of P_{coll} bound to clay colloids or in the NC-bound P_{coll} form once it entered the soil. Zang et al. (2013) and Makris et al. (2006) also pointed out the significance of manure input for the formation of soil colloids. These explanations, which are consistent with our results, indicate that further colloids may originate in soil due to manure or biogas slurry application (see Fig. 5) (Chen and Arai 2020; Meng et al. 2021). In our data, most soils amended with biochar together with, or instead of, manure or biogas slurry had lower P_{coll} contents than those amended with manure or slurry alone (Tables 2 and S2). There are two possible explanations, namely that: biochar absorbs P_{coll} ; and that biochar enhances soil aggregate formation (see Fig. 5), as previously suggested (Li et al. 2019, 2021b; Zhou et al. 2019). Biochar can interact with soil OC and mineral elements (e.g., Fe/Al, Ca, Mg, Si, Mn), which in turn improves soil aggregation and thus reduces soil P_{coll} loss (Li et al. 2019; Wang et al. 2021). This is because the formation of soil aggregates and their stabilisation are closely linked to OC, given that the OC distribution associated with the aggregates determines the OC storage and retention capacity of soils (Kumar et al. 2023). Biochar not only directly absorbs P_{coll} to reduce its losses from the soil solution to the receiving water, but also creates hotspots for microbial communities that simultaneously affect the soil P_{coll} content (Wang et al. 2023).

Regarding the size distribution of P_{coll} , no clear patterns were observed among the three colloidal fractions (i.e., NC, FC, and MC) as a result of organic fertiliser application. This result is consistent with the hypothesis that differences in organic fertiliser application affect the concentration of compounds adsorbed by colloids (i.e., total P_{coll}), while the colloidal composition affects their distribution and morphology (Li et al. 2021b).

3.6 Environmental implications and future perspectives

By jointly investigating the size and distribution of colloidal components in soils amended with organic fertilisers on a regional scale, the current study provides clear

evidence that colloids are important carriers of P. The P_{coll} has a different environmental fate and plays a more active role than other P-forms (particularly dissolved P, in which it is commonly considered) in the P-cycling in soils (Henderson et al. 2012; Lin et al. 2012). Additionally, P_{coll} is often present in association with soil OC and mineral colloids. After its release, its small particles (i.e., NC and FC; <220 nm) can become bioavailable by dissolution or desorption or by diffusion near the plant root (Montalvo et al. 2015; Eltohamy et al. 2023b). While its medium-sized fraction (i.e., MC) forms complexes with other colloids, causing P occlusion and contributing to vertical P-transport into receiving waters (i.e., leaching or runoff) (Konrad et al. 2021; Eltohamy et al. 2023b). Thus, the starting point for studying the colloidal loss potential of a particular soil is to understand the composition of its organic and mineral phases as well as its function (Li et al. 2021b). This is an important prerequisite for formulating an appropriate fertilisation strategy to reduce potential losses of P_{coll} and make it more bioavailable to crops (Eltohamy et al. 2023a). Improving the bioavailability of P_{coll} will help reduce overall organic P-fertilisers in soils to environmentally acceptable levels while maintaining optimal growing conditions for plants.

The results also showed that soils amended with biochar together with, or instead of, manure or biogas slurry had lower P_{coll} levels than soils fertilised with manure or slurry alone. Biochar, as far as we know, is involved in the remediation of pollutants in soils via a variety of processes, either directly by immobilising pollutants or indirectly by affecting soil metabolic activities and degradation (Li et al. 2022; Xiang et al. 2022). Biochar also contributes to carbon neutrality due to its carbon-negative nature, CO_2 sorption, and adverse priming effects (Wang et al. 2023). Moreover, biochar can afford microorganisms' habitats, reduce pollutants' toxicity to microorganisms, and mitigate various biotic and abiotic stresses on plants (Xiang et al. 2022). Overall, biochar offers positive attributes that make it a suitable means of improving soil health and promoting plant growth. In this context, we recommend further research to explore the efficacy of biochar amendments in decreasing the P_{coll} release and loss from agricultural soils and to assess the economic and social viability of local manufacturing of biochar amendments.

4 Conclusion

The present study explored the abundance, size and compositional characteristics of P_{coll} in 12 field sites subjected to long-term application of different organic amendments. The results showed that P_{coll} was the major component of TDP in the tested soils, suggesting that the mobile colloidal phase acts as a P carrier, increasing the

potential risk of P transport from these soils to receiving waters. It should also be highlighted that the soils amended with biochar showed lower P_{coll} contents than those amended with manure or slurry alone, and this effect should be further explored in a controlled inductive research approach. In the three colloidal fractions, OC_{coll} was the major colloid component for P-binding in these soils, with varying contributions from the other colloidal elements. In the NC fraction, the OC–Ca associations were the major vectors for NC-bound P_{coll} . In contrast, MC-bound P_{coll} was better associated with OC–Mn/Fe/Al colloids than with OC–Ca colloids. In the FC fraction, both phenomena (i.e., OC–Ca–P and OC–Mn/Fe/Al–P) occurred together. It can be concluded that the compositions of P_{coll} in different size fractions in soils amended with organic fertilisers are different. Therefore, the starting point for studying the colloidal loss potential of a particular soil enriched with organic fertiliser is to understand the composition of its colloidal organic and mineral phases as well as their function in the soil solution. This study adds to the understanding of how P_{coll} of different size fractions behaves in soils enriched with different organic amendments. As such, it offers valuable insights for the formulation of future policies and the development of pertinent agronomic and environmental strategies.

Abbreviations

P	Phosphorus
TDP	Total dissolved P in soil solution (< 450 nm)
P_{coll}	Colloidal P (in the size range of ~1 (3 kDa)–450 nm)
TSP	Truly soluble P (< 3 kDa)
NC	Nano-sized colloids (~ 1–20 nm)
FC	Fine-sized colloids (~ 20–220 nm)
MC	Medium-sized colloids (~ 220–450 nm)
OC_{coll}	Colloidal organic carbon
Al_{coll}	Colloidal aluminium
Fe_{coll}	Colloidal iron
Mg_{coll}	Colloidal magnesium
Ca_{coll}	Colloidal calcium
Si_{coll}	Colloidal silicon
Mn_{coll}	Colloidal manganese
CEC	Cation exchange capacity
MWHC	Maximum water-holding capacity
DLS	Dynamic light scattering
DPi	Dissolved molybdate-reactive P (dissolved inorganic P)
DPo	Dissolved molybdate-unreactive P (dissolved organic P)
Pi_{coll}	Colloidal molybdate-reactive P_{coll} (colloidal inorganic P)
Po_{coll}	Colloidal molybdate-unreactive P (colloidal organic P)
PCA	Principal component analysis
Q^2	Model cross-validation
PLS-DA	Partial least squares-discriminant multivariate analysis

Supplementary Information

The online version contains supplementary material available at <https://doi.org/10.1007/s44246-023-00048-2>.

Additional file 1. Supplementary Materials.

Acknowledgements

We acknowledge the National Natural Science Foundation of China, the Bingtuan Science and Technology Program, the Natural Science Foundation of Zhejiang Province, and the Key Laboratory of Environment Remediation and Ecological Health, Ministry of Education, College of Environmental and Resource Sciences, Zhejiang University.

Authors' contributions

Kamel Mohamed Eltohamy: Conceptualization, Methodology, Software, Validation, Formal analysis, Investigation, Data Curation, Writing- Original draft, Visualization, Writing—Review & Editing. Paul J. Milham: Investigation, Writing—Review & Editing. Mostafa Gouda: Writing—Review & Editing. Daniel Menezes-Blackburn: Writing—Review & Editing. Sangar Khan: Writing—Review & Editing. Liu Boyi: Writing—Review & Editing. Jin Junwei: Writing—Review & Editing. Xinqiang Liang: Supervision, Project administration, Funding acquisition. The author(s) read and approved the final manuscript.

Funding

We are grateful for the financial support through the grants from the National Natural Science Foundation of China (42277005; 22076163; 41522108), the Bingtuan Science and Technology Program (2021DB019), and the Natural Science Foundation of Zhejiang Province (LR16B070001).

Availability of data and materials

The datasets of this study are available upon request from the corresponding author on reasonable request.

Declarations

Competing interests

The authors declare no competing financial interests.

Author details

¹Key Laboratory of Environment Remediation and Ecological Health, Ministry of Education, College of Environmental and Resource Sciences, Zhejiang University, Hangzhou 310058, China. ²Department of Water Relations & Field Irrigation, National Research Centre, Dokki 12622, Cairo, Egypt. ³Hawkesbury Institute for the Environment, University of Western Sydney, LB 1797, Penrith, New South Wales 2751, Australia. ⁴Department of Nutrition & Food Science, National Research Centre, Dokki 12622, Cairo, Egypt. ⁵Department of Soils, Water and Agricultural Engineering, Sultan Qaboos University, Al-Khoud 123, PO Box 34, Muscat, Sultanate of Oman. ⁶Sino-Japan Friendship Centre for Environmental Protection, Beijing 100029, China.

Received: 19 December 2022 Revised: 24 February 2023 Accepted: 19 March 2023

Published online: 06 April 2023

References

- Adediran GA, Lundberg D, Almkvist G, Pradas del Real AE, Klysubun W, Hillier S, Gustafsson JP, Simonsson M (2021) Micro and nano sized particles in leachates from agricultural soils: Phosphorus and sulfur speciation by X-ray micro-spectroscopy. *Water Res* 189:116585
- Baalousha M, Kammer FVD, Motelica-Heino M, Le Coustumer P (2005) 3D characterization of natural colloids by FIFFF-MALLS-TEM. *Anal Bioanal Chem* 383:549–556
- Baken S, Moens C, van der Grift B, Smolders E (2016a) Phosphate binding by natural iron-rich colloids in streams. *Water Res* 98:326–333
- Baken S, Regelink IC, Comans RNJ, Smolders E, Koopmans GF (2016b) Iron-rich colloids as carriers of phosphorus in streams: A field-flow fractionation study. *Water Res* 99:83–90
- Chen A, Arai Y (2020) Current uncertainties in assessing the colloidal phosphorus loss from soil. Elsevier Inc.,
- Das PP, Singh KRB, Nagpure G, Mansoori A, Singh RP, Ghazi IA, Kumar A, Singh J (2022) Plant-soil-microbes: A tripartite interaction for nutrient acquisition and better plant growth for sustainable agricultural practices. *Environ Res* 214:113821

- Eltohamy KM, Khan S, He S, Li J, Liu C, Liang X (2023a) Prediction of nano, fine, and medium colloidal phosphorus in agricultural soils with machine learning. *Environ Res* 220:115222
- Eltohamy KM, Li J, Gouda M, Menezes-Blackburn D, Milham PJ, Khan S, Li F, Liu C, Xu J, Liang X (2023b) Nano and fine colloids suspended in the soil solution regulate phosphorus desorption and lability in organic fertilizer-amended soils. *Sci Total Environ* 858:160195
- Eltohamy KM, Liu C, Khan S, Niyungeko C, Jin Y, Hosseini SH, Li F, Liang X (2021) An internet-based smart irrigation approach for limiting phosphorus release from organic fertilizer-amended paddy soil. *J Clean Prod* 293:126254
- Fresne M, Jordan P, Fenton O, Mellander PE, Daly K (2021) Soil chemical and fertilizer influences on soluble and medium-sized colloidal phosphorus in agricultural soils. *Sci Total Environ* 754:142112
- García-Gaines RA, Frankenstein S (2015) USCS and the USDA Soil Classification System: Development of a mapping scheme. US Army Eng Res Dev Center, Cold Reg Res Eng Lab
- Gottselig N, Nischwitz V, Meyn T, Amelung W, Bol R, Halle C, Vereecken H, Siemens J, Klumpp E (2017) Phosphorus Binding to Nanoparticles and Colloids in Forest Stream Waters. *Vadose Zo J* 16:16.vzj2016.07.0064
- Gottselig N, Sohr J, Uhlir D, Nischwitz V, Weiler M, Amelung W (2020) Groundwater controls on colloidal transport in forest stream waters. *Sci Total Environ* 717:134638
- Gu S, Gruau G, Dupas R, Jeanneau L (2020) Evidence of colloids as important phosphorus carriers in natural soil and stream waters in an agricultural catchment. *J Environ Qual* 49:921–932
- Henderson R, Kabengi N, Mantripragada N, Cabrera M, Hassan S, Thompson A (2012) Anoxia-induced release of colloid- and nanoparticle-bound phosphorus in grassland soils. *Environ Sci Technol* 46:11727–11734
- Hens M, Merckx R (2002) The role of colloidal particles in the speciation and analysis of “dissolved” phosphorus. *Water Res* 36:1483–1492
- Hosseini SH, Liang X, Niyungeko C, Miaomiao H, Li F, Khan S, Eltohamy KM (2019) Effect of sheep manure-derived biochar on colloidal phosphorus release in soils from various land uses. *Environ Sci Pollut Res* 26:36367–36379
- Jiang X, Bol R, Cade-Menun BJ, Nischwitz V, Willbold S, Bauke S, Vereecken H, Amelung W, Klumpp E (2017) Colloid-bound and dissolved phosphorus species in topsoil water extracts along a grassland transect from Cambisol to Stagnosol. *Biogeosciences* 14:1153–1164
- Jiang X, Bol R, Nischwitz V, Siebers N, Willbold S, Vereecken H, Amelung W, Klumpp E (2015) Phosphorus Containing Water Dispersible Nanoparticles in Arable Soil. *J Environ Qual* 44:1772–1781
- Jin J, Fang Y, He S, Liu Y, Liu C, Li F, Khan S, Eltohamy KM, Liu B, Liang X (2023) Improved phosphorus availability and reduced degree of phosphorus saturation by biochar-blended organic fertilizer addition to agricultural field soils. *Chemosphere* 317:137809
- Julich D, Julich S, Feger K-H (2017) Phosphorus in Preferential Flow Pathways of Forest Soils in Germany. For 8:
- Khan S, Liu C, Milham PJ, Eltohamy KM, Hamid Y, Jin J, He M, Liang X (2022a) Nano and Micro Manure Amendments Decrease Degree of Phosphorus Saturation and Colloidal Phosphorus Release from Agriculture Soils. *SSRN Electron J* 845:157278
- Khan S, Milham PJ, Eltohamy KM, Hamid Y, Li F, Jin J, He M, Liang X (2022b) *Pteris vittata* plantation decrease colloidal phosphorus contents by reducing degree of phosphorus saturation in manure amended soils. *J Environ Manage* 304:114214
- Khan S, Milham PJ, Eltohamy KM, Jin Y, Wang Z, Liang X (2021) Phytate exudation by the roots of *Pteris vittata* can dissolve colloidal $FePO_4$. *Environ Sci Pollut Res* 29:13142–13153
- Konrad A, Billiy B, Regenbogen P, Bol R, Lang F, Klumpp E, Siemens J (2021) Forest Soil Colloids Enhance Delivery of Phosphorus Into a Diffusive Gradient in Thin Films (DGT) Sink. *Front for Glob Chang* 3:1–11
- Kumar D, Purakayastha TJ, Das R, Yadav RK, Shivay YS, Jha PK, Singh S, Aditi K, Prasad PVV (2023) Long-Term Effects of Organic Amendments on Carbon Stability in Clay–Organic Complex and Its Role in Soil Aggregation. *Agronomy* 13:
- Liang X, Jin Y, Zhao Y, Wang Z, Yin R, Tian G (2016) Release and migration of colloidal phosphorus from a typical agricultural field under long-term phosphorus fertilization in southeastern China. *J Soils Sediments* 16:842–853
- Li F, Jin Y, He S, Jin J, Wang Z, Khan S, Tian G, Liang X (2021a) Use of polyacrylamide modified biochar coupled with organic and chemical fertilizers for reducing phosphorus loss under different cropping systems. *Agric Ecosyst Environ* 310:107306
- Li F, Liang X, Niyungeko C, Sun T, Liu F, Arai Y (2019) Chapter Two - Effects of biochar amendments on soil phosphorus transformation in agricultural soils. In: Sparks D.L.B.T.-A. in A. (eds) Academic Press, pp 131–172.
- Li F, Wang D, You Y, Li G, Eltohamy KM, Khan S, Riaz L (2022) The application of biochar mitigated the negative effects of freeze-thaw on soil and nutrient loss in the restored soil of the alpine mining area. *Front Environ Sci* 10:2207
- Li F, Zhang Q, Klumpp E, Bol R, Nischwitz V, Ge Z, Liang X (2021b) Organic Carbon Linkage with Soil Colloidal Phosphorus at Regional and Field Scales: Insights from Size Fractionation of Fine Particles. *Environ Sci Technol* 55:5815–5825
- Lin P, Chen M, Guo L (2012) Speciation and transformation of phosphorus and its mixing behavior in the Bay of St. Louis estuary in the northern Gulf of Mexico. *Geochim Cosmochim Acta* 87:283–298
- Makris KC, Grove JH, Matocha CJ (2006) Colloid-mediated vertical phosphorus transport in a waste-amended soil. *Geoderma* 136:174–183
- Menezes-Blackburn D, Bol R, Klumpp E, Missong A, Nischwitz V, Haygarth PM (2021) Citric Acid Effect on the Abundance, Size and Composition of Water-Dispersible Soil Colloids and Its Relationship to Soil Phosphorus Desorption: A Case Study. *J Soil Sci Plant Nutr* 21:2436–2446
- Menezes-Blackburn D, Paredes C, Zhang H, Giles CD, Darch T, Stutter M, George TS, Shand C, Lumsdon D, Cooper P, Wendler R, Brown L, Blackwell M, Wearing C, Haygarth PM (2016a) Organic Acids Regulation of Chemical-Microbial Phosphorus Transformations in Soils. *Environ Sci Technol* 50:11521–11531
- Menezes-Blackburn D, Zhang H, Stutter M, Giles CD, Darch T, George TS, Shand C, Lumsdon D, Blackwell M, Wearing C, Cooper P, Wendler R, Brown L, Haygarth PM (2016b) A Holistic Approach to Understanding the Desorption of Phosphorus in Soils. *Environ Sci Technol* 50:3371–3381
- Meng Q, Jin L, Cheng L, Fang J, Lin D (2021) Release and sedimentation behaviors of biochar colloids in soil solutions. *J Environ Sci (china)* 100:269–278
- Missong A, Bol R, Willbold S, Siemens J, Klumpp E (2016) Phosphorus forms in forest soil colloids as revealed by liquid-state ^{31}P -NMR. *J Plant Nutr Soil Sci* 179:159–167
- Missong A, Holzmann S, Bol R, Nischwitz V, Puhlmann H, v. Wilpert K, Siemens J, Klumpp E (2018) Leaching of natural colloids from forest topsoils and their relevance for phosphorus mobility. *Sci Total Environ* 634:305–315
- Montalvo D, Degryse F, McLaughlin MJ (2015) Natural colloidal P and its contribution to plant P uptake. *Environ Sci Technol* 49:3427–3434
- Murphy J, Riley JP (1962) A modified single solution method for the determination of phosphate in natural waters. *Anal Chim Acta* 27:31–36
- Niyungeko C, Liang X, Liu C, Liu Z, wen, Sheteiyw M, Zhang H, Zhou J, Tian G (2018) Effect of biogas slurry application rate on colloidal phosphorus leaching in paddy soil: A column study. *Geoderma* 325:117–124
- Saeed H, Hartland A, Lehto NJ, Baalousha M, Sikder M, Sandwell D, Mucalo M, Hamilton DP (2018) Regulation of phosphorus bioavailability by iron nanoparticles in a monomictic lake. *Sci Rep* 8:1–14
- Sato S, Solomon D, Hyland C, Ketterings QM, Lehmann J (2005) Phosphorus speciation in manure and manure-amended soils using XANES spectroscopy. *Environ Sci Technol* 39:7485–7491
- Sumner ME, Miller WP (1996) Cation Exchange Capacity and Exchange Coefficients. *Methods Soil Anal* 1201–1229
- Szymańska E, Saccenti E, Smilde AK, Westerhuis JA (2012) Double-check: Validation of diagnostic statistics for PLS-DA models in metabolomics studies. *Metabolomics* 8:3–16
- Wang L, Missong A, Amelung W, Willbold S, Prielzel J, Klumpp E (2020) Dissolved and colloidal phosphorus affect P cycling in calcareous forest soils. *Geoderma* 375:114507
- Wang S, Li T, Zheng Z (2017) Distribution of microbial biomass and activity within soil aggregates as affected by tea plantation age. *Catena* 153:1–8
- Wang X, Eltohamy KM, Liu C, Li F, Fang Y, Kawasaki A, Liang X (2023) Biochar reduces colloidal phosphorus in soil aggregates: The role of microbial communities. *J Environ Manage* 326:116745
- Wang Z, Chen L, Liu C, Jin Y, Li F, Khan S, Liang X (2021) Reduced colloidal phosphorus loss potential and enhanced phosphorus availability by manure-derived biochar addition to paddy soils. *Geoderma* 402:115348
- Wu Z, Wang S, Luo J (2018) Transfer kinetics of phosphorus (P) in macrophyte rhizosphere and phytoremoval performance for lake sediments using DGT technique. *J Hazard Mater* 350:189–200
- Xia B, Qiu H, Knorr KH, Blodau C, Qiu R (2018) Occurrence and fate of colloids and colloid-associated metals in a mining-impacted agricultural soil upon prolonged flooding. *J Hazard Mater* 348:56–66

- Xiang L, Harindintwali JD, Wang F, Redmile-Gordon M, Chang SX, Fu Y, He C, Muhoza B, Brahushi F, Bolan N, Jiang X, Ok YS, Rinklebe J, Schaeffer A, Zhu Y, Tiedje JM, Xing B (2022) Integrating Biochar, Bacteria, and Plants for Sustainable Remediation of Soils Contaminated with Organic Pollutants. *Environ Sci Technol* 56:16546–16566
- Yan J, Jiang T, Yao Y, Lu S, Wang Q, Wei S (2016) Preliminary investigation of phosphorus adsorption onto two types of iron oxide-organic matter complexes. *J Environ Sci* 42:152–162
- Yang B, Lin H, Bartlett SL, Houghton EM, Robertson DM, Guo L (2021a) Partitioning and transformation of organic and inorganic phosphorus among dissolved, colloidal and particulate phases in a hypereutrophic freshwater estuary. *Water Res* 196:117025
- Yang L, Wu Y, Wang Y, An W, Jin J, Sun K, Wang X (2021b) Effects of biochar addition on the abundance, speciation, availability, and leaching loss of soil phosphorus. *Sci Total Environ* 758:143657
- Yu G, Xiao J, Hu S, Polizzotto ML, Zhao F, McGrath SP, Li H, Ran W, Shen Q (2017) Mineral Availability as a Key Regulator of Soil Carbon Storage. *Environ Sci Technol* 51:4960–4969
- Zang L, Tian GM, Liang XQ, He MM, Bao QB, Yao JH (2013) Profile distributions of dissolved and colloidal phosphorus as affected by degree of phosphorus saturation in paddy soil. *Pedosphere* 23:128–136
- Zhao K, Wang N, Jiang S, Li F, Luo S, Chen A, Li H, Lin X (2022) Potential implications of biochar and compost on the stoichiometry - based assessments of soil enzyme activity in heavy metal - polluted soils. *Carbon Res* 1:1–19
- Zhejiang Soil Census Office (1994) *Soil of Zhejiang*. Zhejiang Science and Technology Press, Hangzhou, China
- Zhou J, Liang X, Shan S, Yan D, Chen Y, Yang C, Lu Y, Niyungeko C, Tian G (2019) Nutrient retention by different substrates from an improved low impact development system. *J Environ Manage* 238:331–340

Publisher's Note

Springer Nature remains neutral with regard to jurisdictional claims in published maps and institutional affiliations.